Applied Surface Science 311 (2014) 5–8

Contents lists available at ScienceDirect

Applied Surface Science

journal homepage: www.elsevier.com/locate/apsusc

Transport properties of polycrystalline boron doped diamond

J.R. de Oliveira [a], O.M. Berengue [b], J. Moro [c], N.G. Ferreira [a], A.J. Chiquito [d], M.R. Baldan [a,*]

[a] Instituto Nacional de Pesquisas Espaciais, INPE/LAS, S.J. Campos, SP 12227-010, Brazil
[b] Universidade Estadual Paulista, UNESP Departamento de Física, Guaratinguetá 12.516-410, Brazil
[c] Instituto Federal de Educação, Ciência e Tecnologia de São Paulo, Bragança Paulista 12929-600, Brazil
[d] Universidade Federal de São Carlos, Departamento de Física, São Carlos 13565-905, Brazil

ARTICLE INFO

Article history:
Received 19 November 2013
Received in revised form 15 April 2014
Accepted 22 April 2014
Available online 27 May 2014

Keywords:
Diamond
BDD
Hall effect

ABSTRACT

The influence of doping level in the electronic conductivity and resistivity properties of synthetic diamond films grown by hot filament chemical vapor deposition (HFCVD) was investigated. Eight different doping level concentrations varied from 500 to 30,000 ppm were considered. The polycrystalline morphology observed by scanning electron microscopy and Raman spectra was strongly affected by the addition of boron. The electric characterization by Hall effect as a function of temperature and magnetic field showed that at sufficiently low temperatures, electrical conduction is dominated by variable range hopping (VRH) conducting process. The resistivity was also investigated by temperature-dependent transport measurements in order to investigate the conduction mechanism in the doped samples. The samples exhibited the VRH ($m = 1/4$) mechanism in the temperature range from 77 to 300 K. The interface between metal, and our HFCVD diamond was also investigated for the lower doped samples.

1. Introduction

Because of the superior properties of diamond, chemical vapor-deposition diamond films have attracted great attention in various applications to electronic and optoelectronic devices. Diamond, although an insulator with a band gap of 5.4 eV can be considered an extrinsic semiconductor material by the addition of low doping levels of boron that leads to a p-type semiconductor. At high doping levels, the diamond acts as a semimetal. Because of its large band gap and its low carrier activation energy of 0.37 eV, the diamond represents an ideal system for studying hopping conduction. For electronic application, boron has been therefore, widely studied as a p-type dopant in diamond. Boron is incorporated substitutionally via replacement of a carbon atom, and is currently the most successful used as acceptor in diamond. Boron doped diamond (BDD) has also emerged as an attractive material because its electrochemical properties such as low background current, wide potential window, and good response to redox species [1].

At relative high temperatures, the conduction in the valence band becomes negligible allowing the study the hopping conduction [2]. Besides, the dopant presents a small Bohr radius meaning that metallic conduction only begins at higher concentration (10^{20} cm^{-3}).

2. Experimental details

The diamond films depositions were grown on polished silicon (1 0 0) 1 cm × 1 cm samples in a conventional hot filament chemical vapor deposition HFCVD reactor using the following growth parameters: temperature of 900 K, pressure of 4.0 kPa and deposition time of 10 h. The CH_4 concentration was kept constant in 1.0 vol.% and the 99 vol.% of H_2, the total gas flow was 200 sccm. Five filaments of tungsten were used, and their temperature during the experiment was around 2300 K. The substrates were prepared by ultrasonic hexane bath with 0.25 μm diamond powder during 60 min and the diamond films were deposited in two phases. In the first phase was grown an insulating microcrystalline diamond film. In the second phase was grown boron diamond film. The boron doping concentration varied from 500 to 30,000 ppm.

The boron doping was performed by addition B_2O_3 to the CH_3OH in the bubbler. When B_2O_3 is dissolved in CH_3OH, trimethylborate $(CH_3O)_3B$ is produced, and it is the substance containing boron that is added to the gas mixture during the growth process. The solution was prepared with concentration of B_2O_3 dissolved in CH_3OH from 500 to 30,000 ppm of boron atoms in relation to the carbon atoms of the CH_3OH (B/C ratios). The volume of CH_3OH was fixed at 200 mL for all solutions. Each solution was placed in a bubbler at a constant

* Corresponding author. Tel.: +55 12 32086560.
E-mail addresses: baldan@las.inpe.br, mrbaldan@uol.com.br (M.R. Baldan).

http://dx.doi.org/10.1016/j.apsusc.2014.04.161
0169-4332/

pressure and temperature, and the H_2 gas was used as a carrier with a constant flow of 30 sccm.

The morphologies of the films were analyzed by scanning electron microscopy (SEM) using a JEOL JSM-5310 model, and the quality of films was evaluated by micro-Raman scattering spectroscopy (Renishaw microscope system 2000) using the 514.5 nm line of an argon ion laser, taking the spectra covering the range from 300 to 3500 cm^{-1}. In order to verify the conduction mechanism of diamond films, it was used on ac conductivity/resistivity measurements in the Van der Pawn geometry [3] which was used to Hall measurements as well. As-grown CVD diamond usually has hydrogenated surfaces that behave as a p-type semiconductor, and must be removed by cleaning the diamond in oxidizing reagents. Then, before device fabrication, the samples were initially treated with a conventional degrease solution based on trichloroethylene followed by acetone; next, the samples were immersed in a saturated solution of H_2SO_4/K_2CrO_4 at 200 °C for 2 h and immediately rinsed in NH_4OH/H_2O_2 solution and deionized water. The electrical contacts were obtained by metallization (Ti/Au, 50 nm/100 nm) in a high vacuum chamber (10^{-6} Torr) using shadow masks; the devices were then annealed in Ar atmosphere at 600 °C during 10 min. When Schottky devices were needed 100 nm thick aluminum contacts were used.

Some Hall measurements conducted immediately after the cleaning process above described lead to unexpected results (all samples presented almost the same density of carriers). Then we decided to clean them again in the same route, but the samples were exposed to an oxygen plasma (50 W, 10 min) before making electrical contacts. Fig. 1 depicts the effect of the plasma cleaning in the Hall data for the lower doped sample (500 ppm). Before plasma cleaning all different doped samples presented the same carrier density. After plasma treatment, we are really probing the diamond film without hydrogenated surfaces, which have affected the previous results.

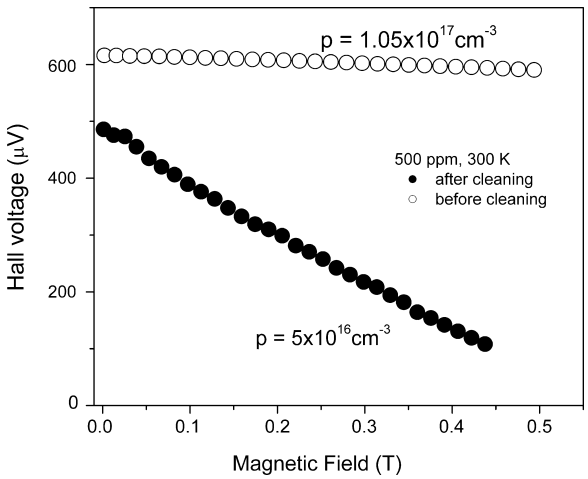

Fig. 1. Hall data before and after the cleaning process using chemical and oxygen plasma cleaning. Before plasma cleaning all different doped samples presented the same carrier density. After plasma treatment we are really probing the diamond film without hydrogenated surfaces which have affected the previous results.

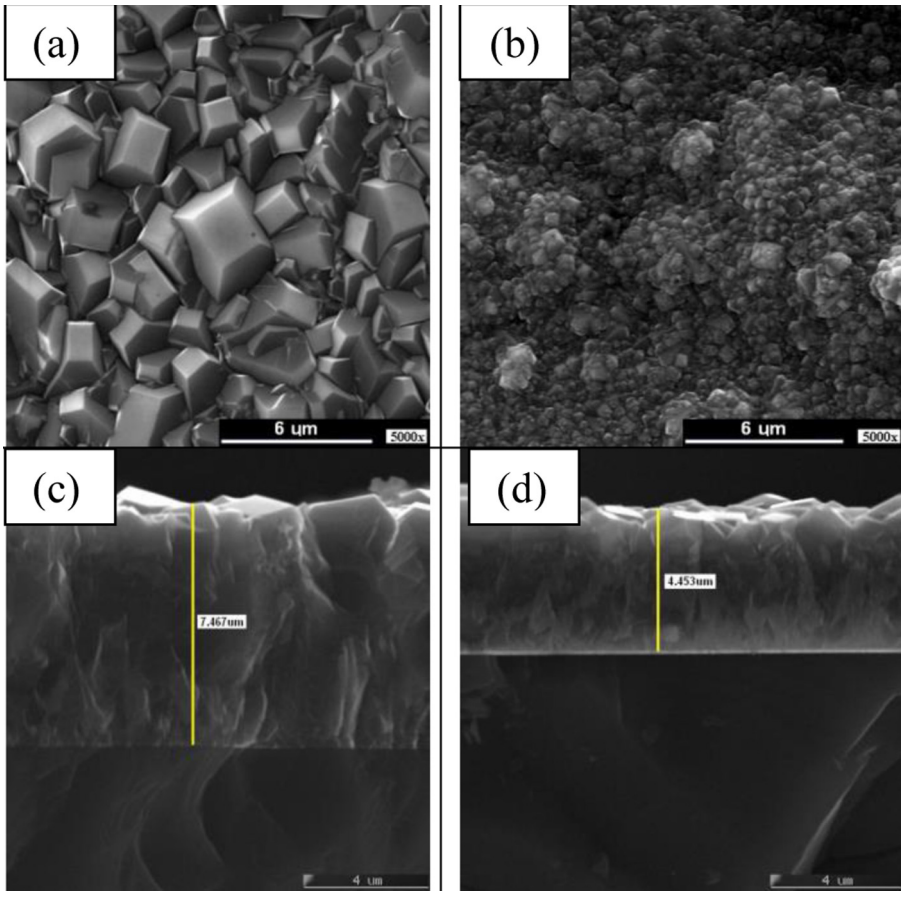

Fig. 2. Scanning electron microscopy (SEM) images of the samples doped with (a) 500 ppm and (b) 30,000 ppm. SEM cross-section of the diamond (c) 500 ppm and (d) 30,000 ppm.

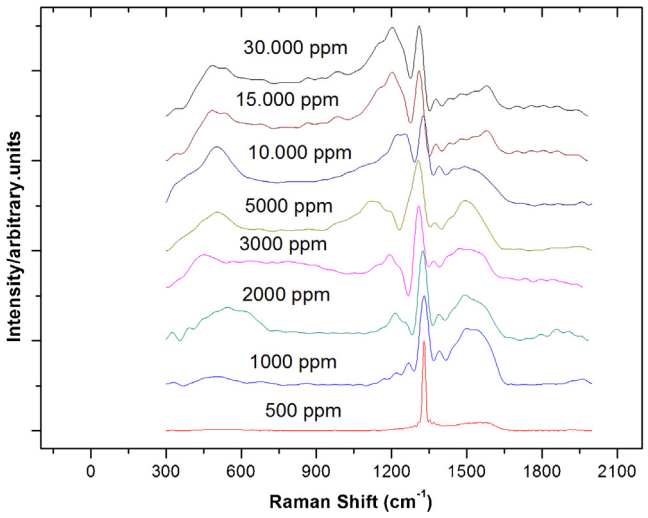

Fig. 3. Raman spectra for all the samples from 500 cm^{-1} to 30,000 cm^{-1}.

3. Results and discussion

Micrographs obtained by SEM showed that there was a significant change in diamond grains size and films surface morphology with the continuous addition of boron. The images show that as the boron content increases from 500 ppm to 30,000 ppm the microstructure is continuously changing from well-shape grains (500 ppm Fig. 2a) to a smoothness ball-like structure composed of clusters of tiny grains (30,000 ppm Fig. 2b) frequently denominated as cauliflower-like structure, also typical of NCD films. The films grown in the range from 500 ppm to 10,000 ppm present a typical dominant structure with crystal orientation composed by a mixture of (1 1 1) and (1 0 0).

The morphologic changes observed by SEM analysis are also reflected on the Raman spectra features Fig. 3. This spectra showed the characteristic Raman peak of diamond (sp^3-bonded carbon) at 1332 cm^{-1}, and this peak is well defined for all the samples investigated. The measurements are characterized by two broad bands at 500 and 1230 cm^{-1}. The presence of the 500 cm^{-1} is attributed to the concentration increase in the boron pairs that have local vibration modes giving wide bands around 500 cm^{-1}. In addition, there is the appearance of the t bands located at 1220 cm^{-1} [4]. More recently, Niu et al. [5] have discussed the electronic and vibrational properties of heavily BDD. They concluded that the 500 and ~1220 cm^{-1} bands are both superposed bands, including not only C vibrations but also B–B vibrations and B–C vibrations, respectively. It is important to notice the evolution of doping concentration from 500 to 30,000 ppm. For the lowest concentration, at 500 ppm, the peak at 1332 cm^{-1} is well defined, besides it is not observed in the band at 500 cm^{-1}. For the films doped above 500 ppm, the spectrum started to present some significant changes as a function of doping level. The effect of doping can be verified by looking at the evolution of the band at 1200 cm^{-1} that increases as a function of the boron incorporated into the diamond lattice. The increase of this band is a strong indicative that the doping was effective.

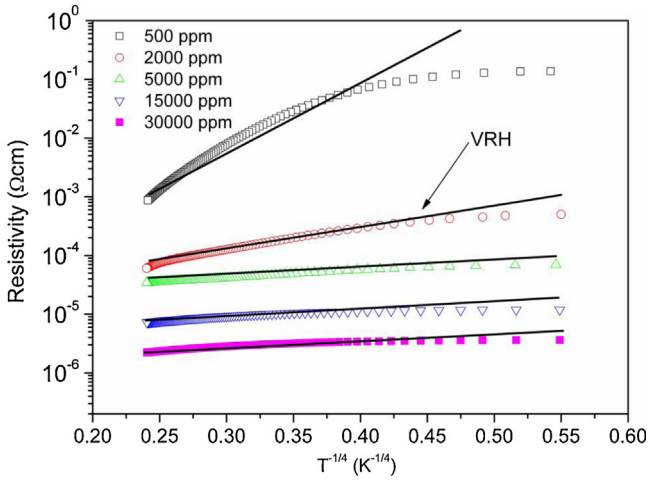

Fig. 4. Temperature dependence of the resistivity of some samples with different boron doping levels.

The resistivity of the samples was also investigated by temperature-dependent transport measurements in order to investigate the conduction mechanism in the doped samples. Several authors have reported that the resistivity in diamond films can be described by the variable range hopping mechanism (VRH), nearest hopping mechanism, and, in some cases, by a thermally activated mechanism [6]. The hopping conduction processes are governed by the well-known equation

$$\rho(T) = \rho_0 \exp\left(\frac{T}{T_0}\right)^m \quad (1)$$

where T_0 is related to the density of states at the Fermi energy and to the localization length. Usually, the VRH ($m = 1/4$) conduction occurs at low temperatures when the excitation energy is not sufficient to surmount the Coulomb gap or when the energy dispersion is large.

The temperature dependence of samples resistivity is depicted in Fig. 4. All the samples exhibited the VRH ($m = 1/4$) mechanism in the temperature range from 77 to 300 K. This result was already expected for lower impurity concentration, when the conduction of carriers (holes) is governed by hopping even in high temperatures. It should be noted that the exponent in Eq. (1) was a fit parameter not a predefined value (1/2 or 1/4) as usually found in literature. Because of the unrealistic values obtained by the fitting process in the very low temperature range, we started it at 20 K. Sato et al. [7] showed that, in this region, a simple activation conduction controls the resistivity of the diamond films. However, when the impurity concentration increases, the wavefunctions of boron overlap forming an impurity band favoring the variable range hopping.

As an additional investigation, we used the lower doped sample for building a diode device in order to characterize the interface between metal and our CVD diamond. A regular metal/semiconductor device is usually described as a diode in which there are two electrical junctions: an ohmic contact presenting linear current–voltage (J–V) characteristic and a rectifying contact, controlled by a potential barrier. However, even using the lower doped sample the depletion region is not large enough to allow us an accurate evaluation of the barrier heights. Then, instead of making ohmic and rectifying contacts, we used two Schottky contacts for simplicity. In order to account the presence of two barriers, the conventional current–voltage equation [8] can be re-written as [9]

$$J(V,T) = \frac{J_{01}J_{02}senh\left(\frac{qV}{2k_BT}\right)}{J_{01}\exp\left(\frac{qV}{2k_BT}\right) - J_{02}\exp\left(\frac{-qV}{2k_BT}\right)},$$

with

$$J_{1,2}(V) = A^*T^2 \exp\left(\frac{q\Phi_{B1,B2}}{k_BT}\right)\left[\exp\left(\frac{qV}{n_{1,2}k_BT}\right) - 1\right]$$

$$= J_{01,02}\left[\exp\left(\frac{qV}{n_{1,2}k_BT}\right) - 1\right] \quad (2)$$

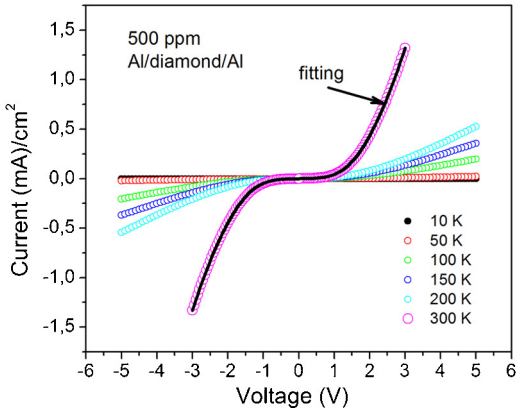

Fig. 5. Current–voltage curves for the lower doped sample at different temperatures. From the back-to-back diodes aspect of these curves, it can be noted promptly the contribution of the two barriers in our devices. The fitting curve is showed only for the 300 K measurement for clearness.

Table 1
Fitting parameters obtained from applying Eq. (1) to the experimental data at different temperatures. The error associated to the barrier height and ideality factor values are 0.01 eV and 0.02, respectively.

T (K)	Φ_{B1} (eV)	Φ_{B2} (eV)	n
10	0.31	0.31	1.02
50	0.29	0.30	1.02
100	0.32	0.31	1.03
150	0.31	0.31	1.03
200	0.31	0.31	1.03
300	0.31	0.31	1.03

where A^* is the Richardson constant, n the ideality factor, Φ_{B1} and Φ_{B2} are the Schottky barriers and the other symbols have their usual meanings.

Fig. 5 depicts the current–voltage curves for the lower doped sample at different temperatures. From the back-to-back diodes aspect of these curves, it can be noted promptly the contribution of the two barriers in our devices. Fitting of Eq. (2) to the experimental data is also plotted in Fig. 5, and the resulting data is shown in Table 1. The agreement of both theoretical and experimental curves in a large range of voltages is quite remarkable. We attribute observation of ideality factors near the unity to the use of the whole current–voltage curve in the fitting procedure. Frequently, the reverse biased junction contribution to the current in a Schottky device is neglected and only the forward contribution of the I–V curves is used for parameters extraction.

In literature, we found barrier heights varying from 0.5 to 1.2 eV for aluminum, but most of the measurements were done in undoped hydrogen terminated diamond surfaces, which produce a p-type surface conductivity (and a negative electron affinity) [10–12]. The large difference observed between barrier height data on literature (themselves) and our results can be addressed to the surface conditions for each measurement.

4. Conclusions

We presented a detailed analysis of the transport properties of boron-doped diamond films grown at different doping levels. A special set of samples was obtained for this purpose. A strong dependence of resistivity on the doping concentration was observed. The variable range hopping (VRH) mechanism seems to be the dominating transport process in a wide range of temperatures. When the impurity concentration increases, the wavefunctions of boron overlap forming an impurity band favoring the variable range hopping. At low doping levels, we were able to determine the barrier height of Schottky devices defined on clean diamond surfaces. In fact, the agreement between the values found here and those in literature allowed us to conclude that the surface cleaning process was effective for all devices developed here.

Acknowledgments

The authors are very grateful to CNPq for the financial support. AJC wishes to thank the Brazilian research funding agencies (Grant 2011/10171-1, Sao Paulo Research Foundation (FAPESP)) and CNPq (Grant 2010/302640-0) for the financial support of this work.

References

[1] I. Yagi, K. Tsunozaki, D.A. Tryk, A. Fujishima, Electrochem. Solid-State Lett. 2 (9) (1999) 457–460.
[2] B. Massarani, J.C. Bourgoin, Hopping conduction in semiconducting diamond, Phys. Rev. B 17 (1978) 1758–1769.
[3] L.J. van der Pauw, Philips Res. Rep. 13 (1958) 1.
[4] P.W. May, W.J. Ludlow, M. Hannaway, P.J. Heard, J.A. Smith, K.N. Rosser, Diamond Related Materials 17 (2008) 105.
[5] L. Niu, J.-Q. Zhu, X. Han, M.-L. Tan, W. Gao, S.-Y. Du, Physics Letter A 373 (2009) 2494.
[6] B. Massarini, J.C. Bourgoin, R.M. Chrenko, Phys. Rev. B 17 (1978) 1758.
[7] T. Sato, K. Ohashi, H. Sugai, T. Sumi, K. Haruna, H. Maeta, N. Matsumoto, H. Otsuka, Phys. Rev. B 61 (2000) 12970.
[8] S.M. Sze, Physics of Semiconductor Devices, Wiley, New York, 1981.
[9] A.J. Chiquito, C.A. Amorim, O.M. Berengue, L.S. Araujo, E.P. Bernardo, E.R. Leite, J. Phys. Condensed Matter 24 (2012) 225303.
[10] C.E. Nebel, B. Rezek, D. Shin, H. Watanabe, Phys. Status Solidi A 203 (2006) 3273.
[11] H. Kiyota, E. Matsushima, K. Sato, H. Okushi, T. Ando, M. Kamo, Y. Sato, M. Iida, Appl. Phys. Lett. 67 (1995) 3596.
[12] K. Tsugawa, H. Noda, K. Hirose, H. Kawarada, Phys. Rev. B 81 (2010) 045303.